

## Electronic supplementary information

### Facet Engineering in Metal Organic Frameworks to Improve Their Electrochemical Activity for Water Oxidation

Jiawei Wan <sup>a,e,f</sup>, Di Liu <sup>b,e</sup>, Hai Xiao <sup>a,\*</sup>, Hongpan Rong <sup>c,\*</sup>, Guan Sheng <sup>d</sup>, Feng Xie <sup>d</sup>,  
Dingsheng Wang <sup>a,\*</sup>, and Yadong Li <sup>a</sup>

<sup>a</sup> Department of Chemistry, Tsinghua University, Beijing, 100084, China

<sup>b</sup> State Key Laboratory of Inorganic Synthesis & Preparative Chemistry, College of Chemistry, Jilin University, Changchun, Jilin 130012, China.

<sup>c</sup> Beijing Key Laboratory of Construction-Tailorable Advanced Functional Materials and Green Applications, School of Materials Science & Engineering, Beijing Institute of Technology, Beijing 100081, China.

<sup>d</sup> Advanced Membranes and Porous Materials Center, Physical Sciences and Engineering Division, King Abdullah University of Science and Technology, Thuwal, 23955-6900, Saudi Arabia.

<sup>e</sup> These authors contributed equally to this paper.

<sup>f</sup> Present address: State Key Laboratory of Biochemical Engineering, Institute of Process Engineering, Chinese Academy of Sciences, Beijing 100190, P. R. China.

\* Corresponding authors:

Email addresses: rhp@bit.edu.cn (H. P. Rong), haixiao@mail.tsinghua.edu.cn (H. Xiao), wangdingsheng@mail.tsinghua.edu.cn (D.S. Wang)

## **Experimental section**

### **1. Chemicals**

Co(NO<sub>3</sub>)<sub>2</sub>·6H<sub>2</sub>O (98%, Alfa), Zn(NO<sub>3</sub>)<sub>2</sub>·6H<sub>2</sub>O (98%, Alfa), 2-methylimidazole (2-MIm, 99%, Acros), ethanol (99.8%, AR grade, Beijing Chemical Reagent Factory), sodium dodecyl sulfate (SDS, 98%, Beijing Chemical Reagent Factory), resorcinol (98%, Beijing Chemical Reagent Factory), Ultrapure water (Millipore Milli-Q grade) with a resistivity of 18.2 MΩ was used in all the experiments. All of the chemicals used in this experiment were used as received without any further purification.

### **2. Synthesis methods**

#### **Synthesis of ZIF-67 nanocrystals**

1.415 g of Co(NO<sub>3</sub>)<sub>2</sub>·6H<sub>2</sub>O was dissolved in 100 ml methanol (solution 1). Then, 1.6 g of 2-MIm was dissolved in another 100 ml methanol (solution 2). Then, the two solutions were mixed together under strongly stirring. After one-hour reaction, the product was collected with centrifugation and washed with deionized water and ethanol for three times, respectively.

#### **Synthesis of 2D ZIF-67 (002):**

First, 1.6 g SDS was completely dissolved in 180 ml ultrapure water under strongly stirring, followed by adding with 1.415 g Co(NO<sub>3</sub>)<sub>2</sub>·6H<sub>2</sub>O. Then, 3.195 g of 2-MIm was well dispersed in 20 ml ultrapure water. Next, the solution of 2-MIm was rapidly injected into the mixture solution. After one-hour reaction, the product was collected with centrifugation and washed with deionized water and ethanol for three times, respectively. The powder was collected by freeze-drying method.

#### **Synthesis of 2D ZIF-8 (002):**

First, 1.6 g SDS was completely dissolved in 180 ml ultrapure water under strongly

stirring, followed by adding with 1.446 g  $\text{Zn}(\text{NO}_3)_2 \cdot 6\text{H}_2\text{O}$ . Then, 3.195 g of 2-MIm was well dispersed in 20 ml ultrapure water. Next, the solution of 2-MIm was rapidly injected into the mixture solution. After one-hour reaction, the product was collected with centrifugation and washed with deionized water and ethanol for three times, respectively. The powder was collected by freeze-drying method.

### **3.Catalyst characterization**

Transmission electron microscopy (TEM) images were performed on a Hitachi H-800 transmission electron microscope. Dark field scanning transmission electron microscopy (DF-STEM) was performed on FEI Tecnai G2 F20 S-Twin high-resolution transmission electron microscope operating at 200kV. The X-ray powder diffraction (XRD) were obtained on a Rigaku RU-200b with  $\text{Cu K}\alpha$  radiation.  $\text{N}_2$  adsorption measurements were performed with a Quantachrome Autosorb-1 instrument surface area analyzer at 77K. The Brunauer-Emmett-Teller (BET) method was used to calculate the specific surface area. The current-voltage (I-V) characteristic of the as-prepared film was examined using a Keithley 2400 sourcemeter.

Samples for TEM measurements were suspended in ethanol and dispersed ultrasonically. Drops of suspensions were applied on a copper grid coated with carbon. HRTEM images were taken on a FEI Titan 60-300 electron microscope equipped with a spherical aberration (Cs) corrector and Gatan K2 direct-detection camera operated in electron-counting mode under 300 kV.

### **4.Electrochemical measurements**

The catalyst ink was prepared by using the mixture of 0.2 ml water, 0.2 ml ethanol, 0.02 ml 5 wt% Nafion solution and 2 mg catalysts followed by ultrasonication for 2h. After that, 10  $\mu$ l of the catalyst ink was uniformly dropped onto the glassy-carbon electrode (diameter of 5 mm). Linear sweep voltammetry (LSV) method was performed in 1.0 M KOH solution in a standard three-electrode system, in which a glassy carbon electrode (GCE) modified with samples, a Pt wire and an Ag/AgCl electrode were used as the working electrode, counter-electrode and reference electrode, respectively. The OER activity of the catalysts was measured by RDE (1200 rpm) with LSV in the potential from 0 to 1.0 V at a scan rate of 10 mV s<sup>-1</sup>.

### **5.DFT parameters**

The calculations were performed with the VASP package<sup>1-3</sup>, using the Perdew-Burke-Ernzerhof (PBE) approximation<sup>4</sup> of density functional theory (DFT) and the projector augmented wave (PAW) method<sup>5</sup> to account for core-valence interactions. The kinetic energy cut-off for plane wave expansions was set to 400 eV, and the reciprocal space was sampled by the  $\Gamma$  point. The convergence criteria are  $1 \times 10^{-5}$  and  $1 \times 10^{-7}$  eV energy differences for solving for the electronic wave function for structure optimization and vibrational frequency calculations, respectively. All atomic coordinates are converged to within  $3 \times 10^{-2}$  eV/Å for maximal components of forces. The zero-point energies (ZPE) and enthalpy and entropy contributions to free energies at room temperature (298.15 K) were all included as described elsewhere<sup>6-7</sup>.

The ZIF-67 (002) surface model was constructed as a 4-layer (1 $\times$ 1) slab, with a vacuum layer of 16 Å. The bottom two layers were fixed to mimic the bulk, with the rest fully relaxed for the structure optimization. We found that Co(II) in the ZIF-67

possesses a high spin  $d^7$  configuration with the tetrahedral splitting, and the ferromagnetic arrangement is favored.

In DFT calculations, the surface coordinatively unsaturated Co atoms act as OER active sites. The deviation of DFT calculations from the experiments is well understood, considering all the assumptions (e.g., perfect surface) and approximations (the GGA of DFT method itself is an approximation that is known to give systematic errors of at least  $\sim 0.2$  eV) made.

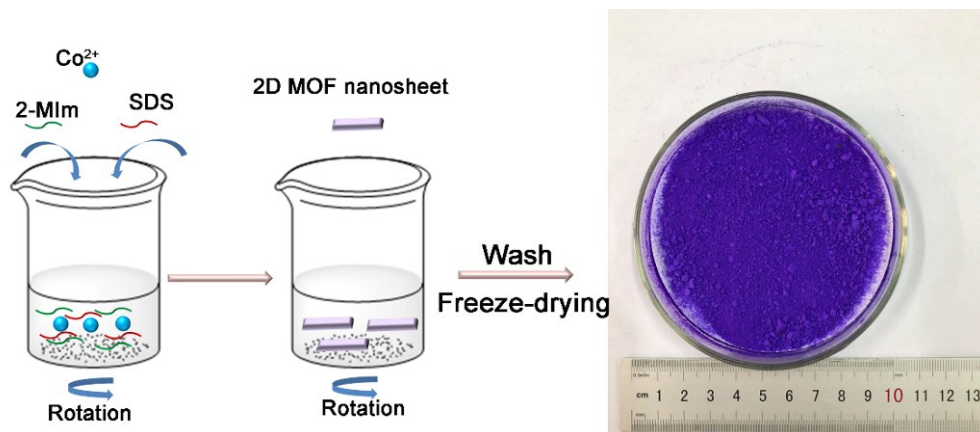


**Figure S1.** Synthetic process of 2D ZIF-67 (002) in water solution at room condition.

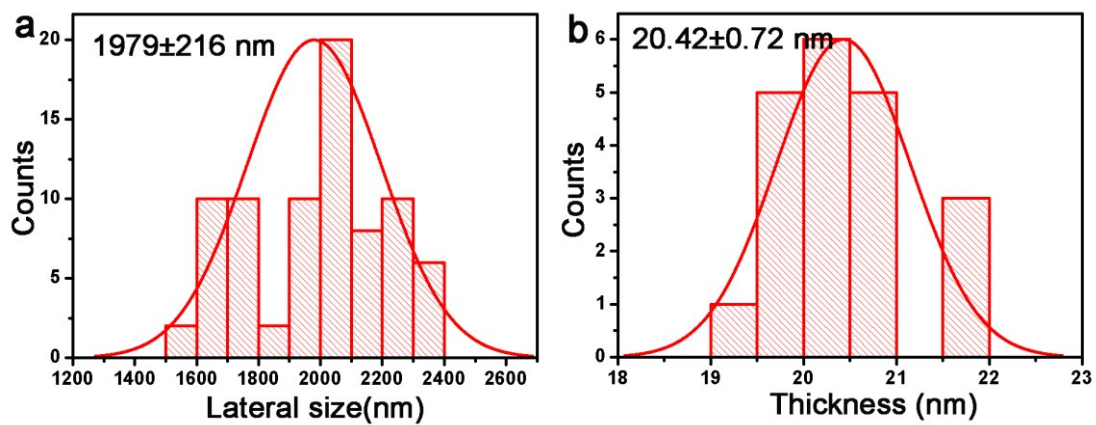


**Figure S2.** Statistical results of (a) lateral size, (b) thickness for ZIF-67 (002).

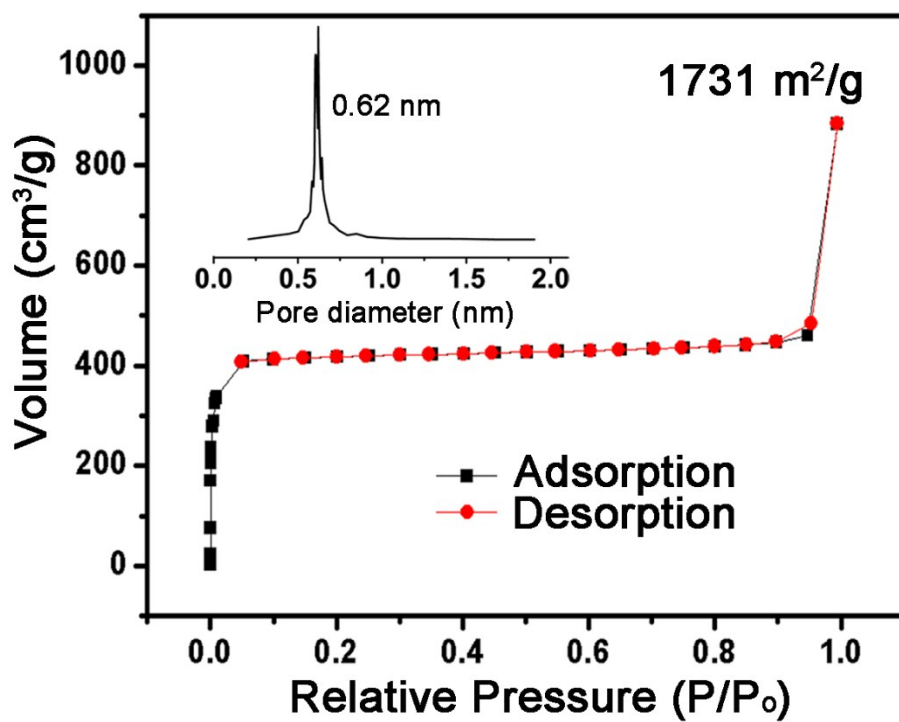


**Figure S3.** N<sub>2</sub> adsorption/desorption isotherms, and pore size distributions of ZIF-67 (002).



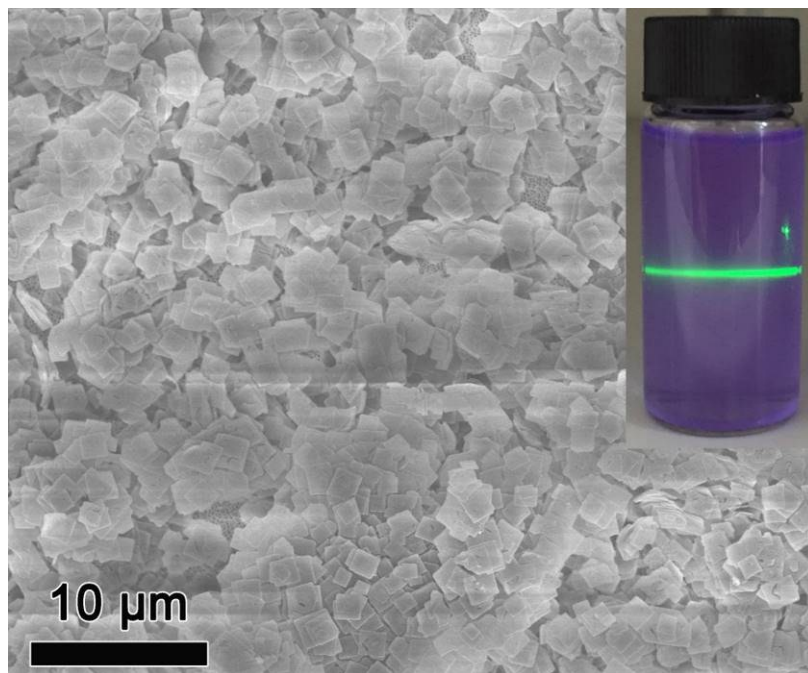


**Figure S4.** SEM image of 2D ZIF-67 (002) and inset is the Tyndall effect of a colloidal solution.

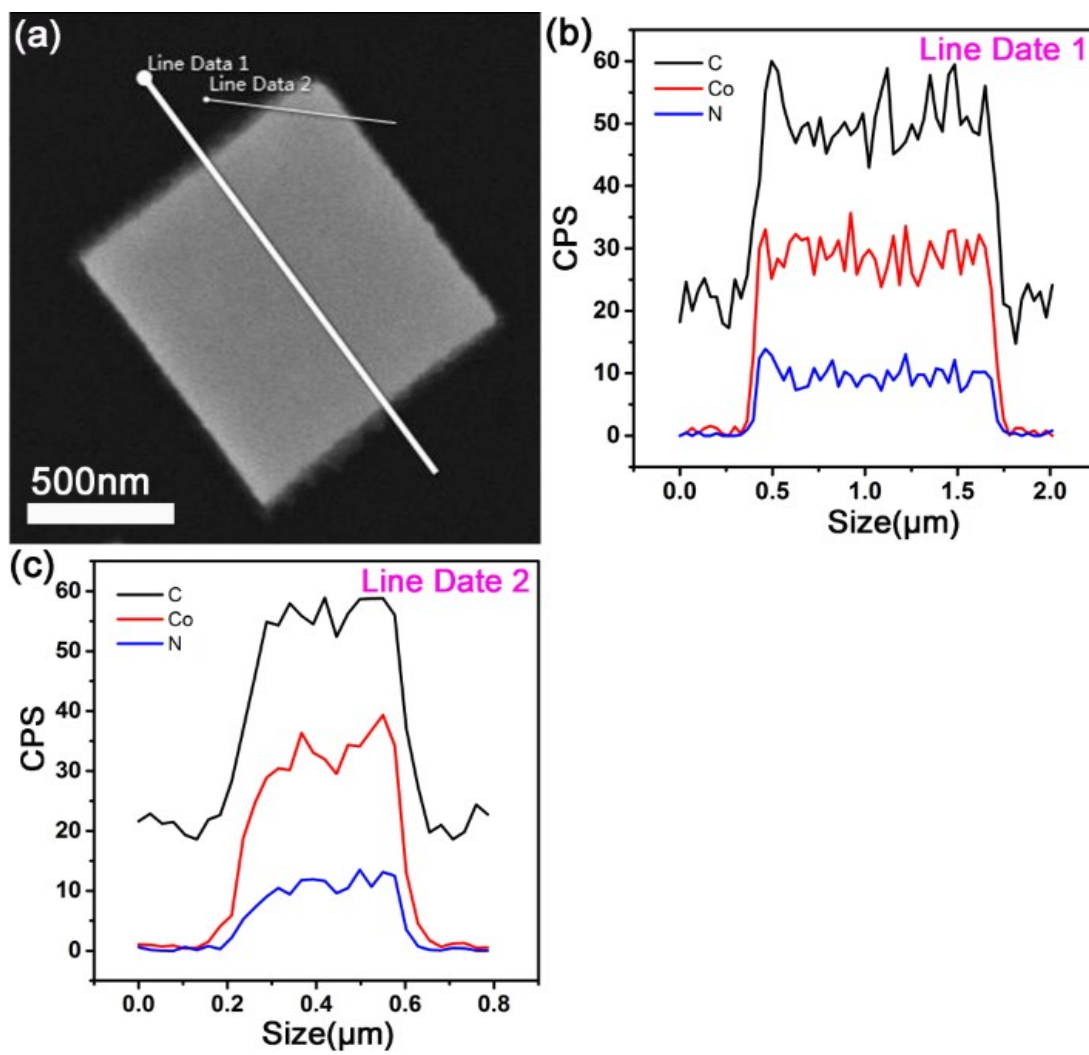


**Figure S5** Line scan results of 2D ZIF-67 (002). (a) TEM image of line 1 and line 2. (b) Elemental distribution for line 1. (c) Elemental distribution for line 2.

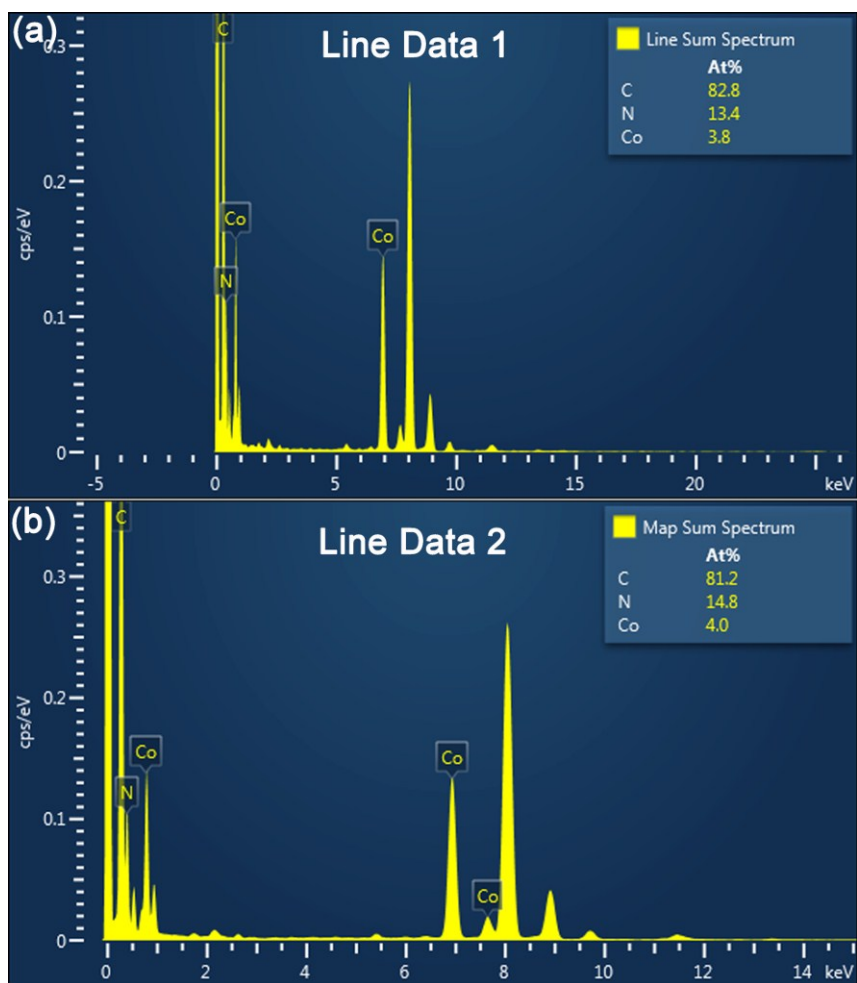


**Figure S6.** EDX results corresponding to Fig. S5. (a) EDX result for line data 1. (b) EDX result for line data 2.

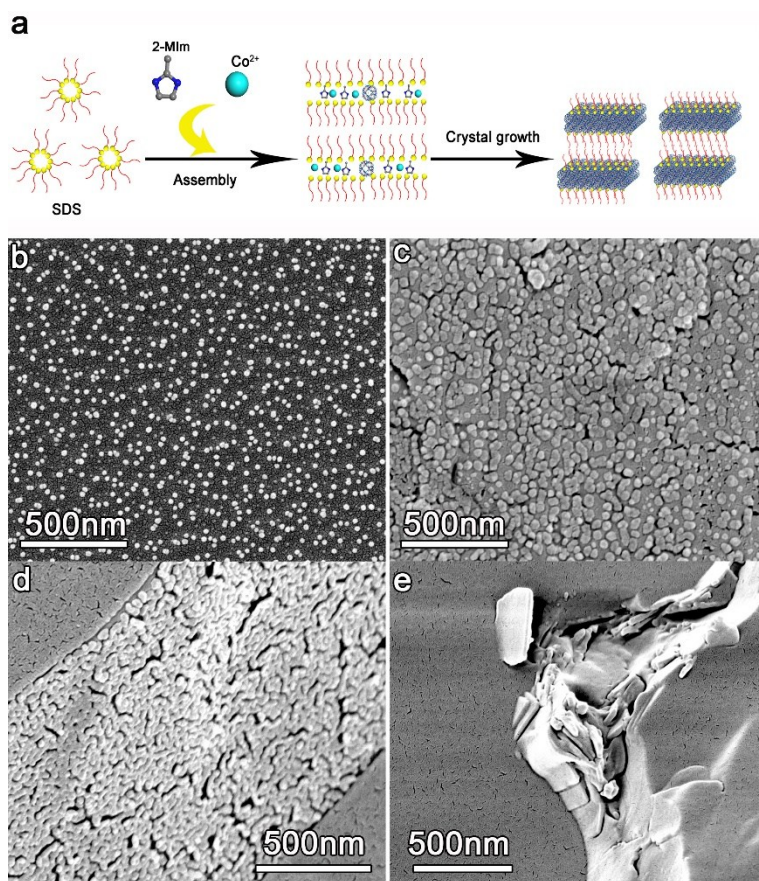


**Figure S7.** Cryo-SEM results for synthetic procedure of ZIF-67 (002). (a) Synthetic procedure of ZIF-67 (002). (b) Cryo-SEM image of SDS solution at the reaction concentration. (c) Mixture solution of SDS and  $\text{Co}(\text{NO}_3)_2$  with same concentration as synthesis process of 2D ZIF-67. (d) Fresh mixture solution of SDS,  $\text{Co}(\text{NO}_3)_2$  and 2-Methylimidazole solution. (e) Mix solution reaction with several minutes.

When SDS reached the reaction concentration of  $5.6 \times 10^{-2} \text{ mol/L}$ , the vesicle structures formed immediately (Fig. S7b). After  $\text{Co}(\text{NO}_3)_2 \cdot 6\text{H}_2\text{O}$  was added and completely dissolved in the above SDS solution, the vesicles grew (Fig. S7c). The same result could be also obtained and confirmed by size distribution from DLS data (Fig. S8). When the 2-MIm solution was immediately added into the above mixture solution (SDS,  $\text{Co}^{2+}$ ), the assembling of vesicles happened and could be recognized in cryo-SEM (Fig. S7d) and DLS results (Fig. S8, green line). After several minutes' growth, the 2D structure could be found in Fig. S7e.

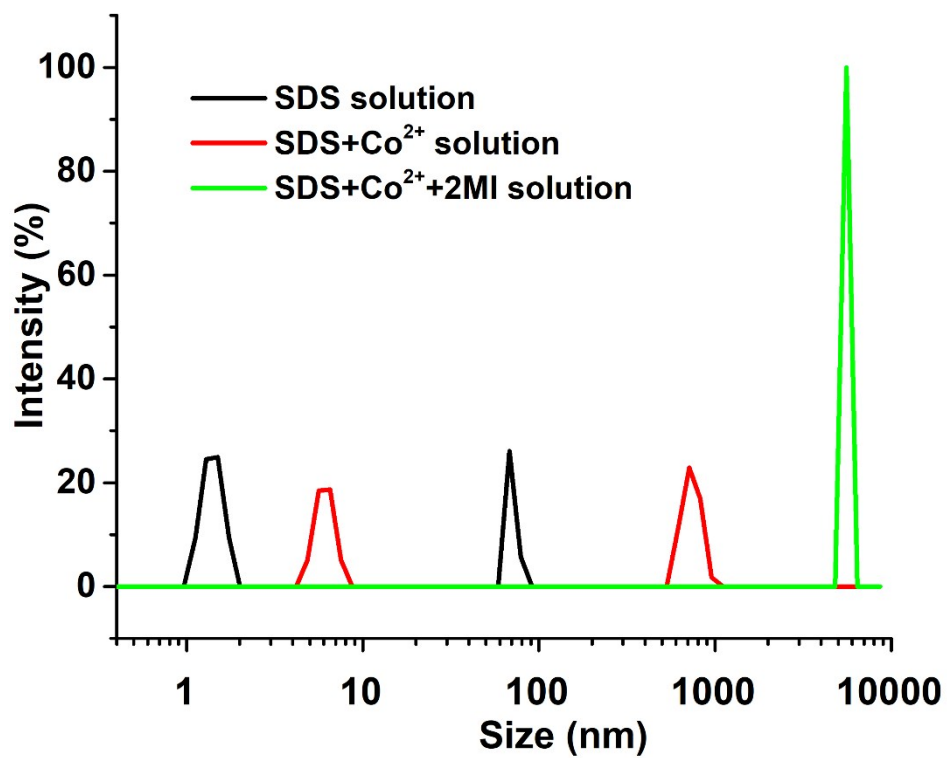


**Figure S8.** Size distribution of the 2D ZIF-67 formation process by dynamic light scattering (DLS) measured at room temperature.

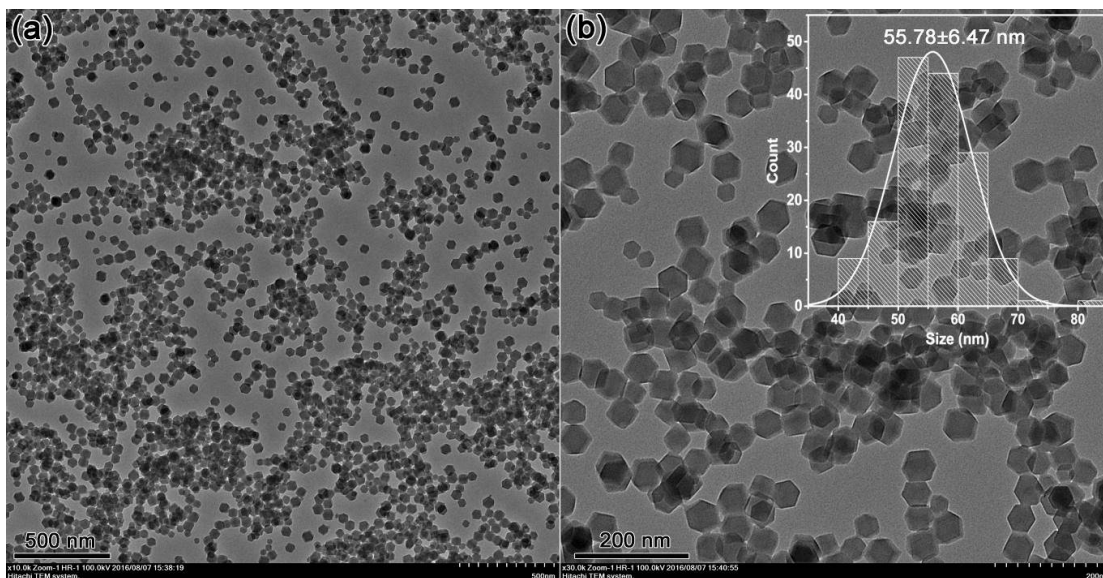


**Figure S9.** TEM results of ZIF-67 nanocrystals. (a) TEM image at small magnification. (b) TEM image at large magnification, corresponding inset is the statistical result of nanocrystal size.

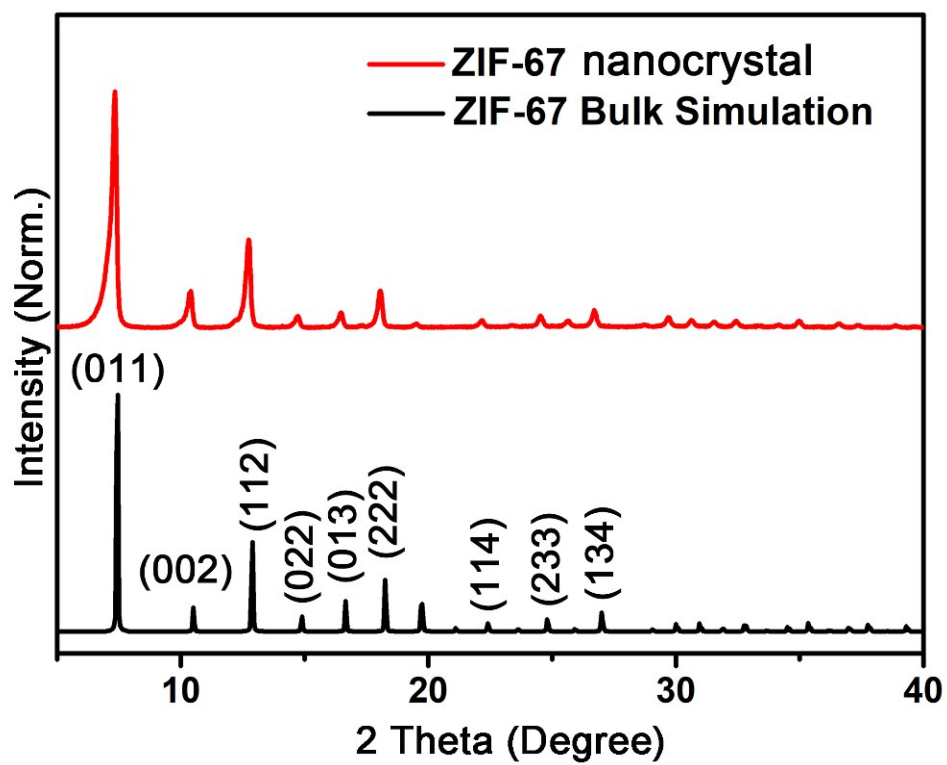


**Figure S10.** XRD patterns of simulated bulk-ZIF-67 and ZIF-67 nanocrystals.

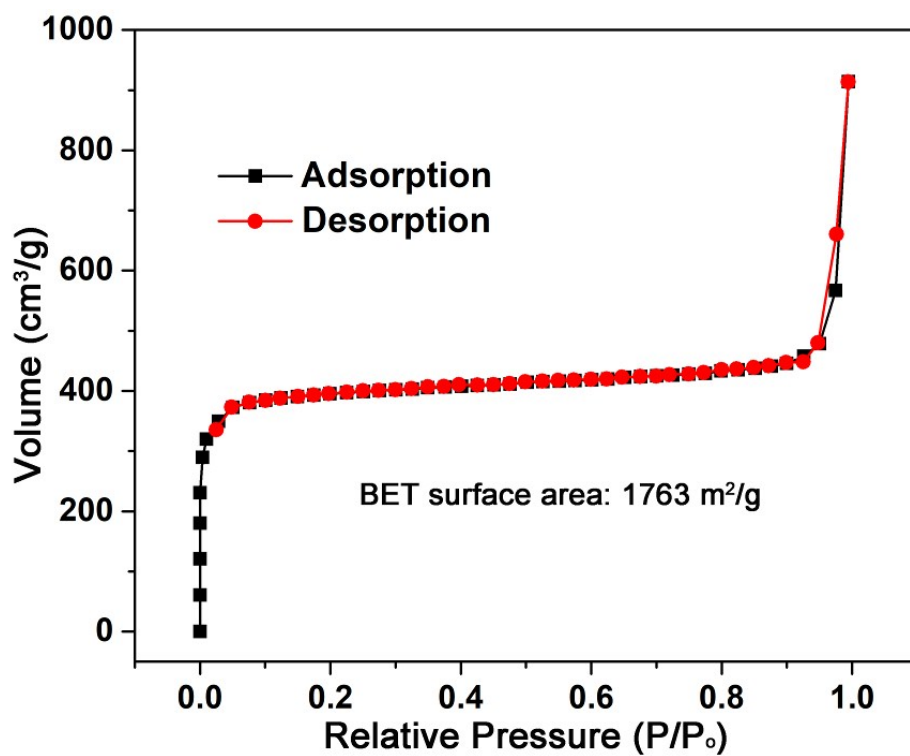


**Figure S11.** N<sub>2</sub> adsorption/desorption isotherms of ZIF-67 nanocrystal. The BET surface area is 1763 m<sup>2</sup>/g.



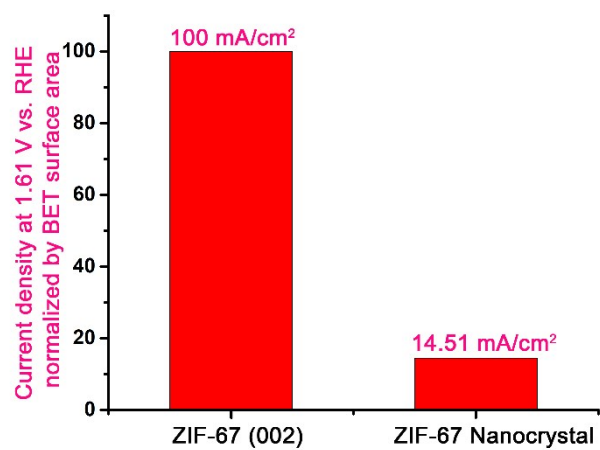


**Figure S12.** The OER current densities at 1.61 V vs. RHE are normalized by the BET surface areas of the two catalysts.

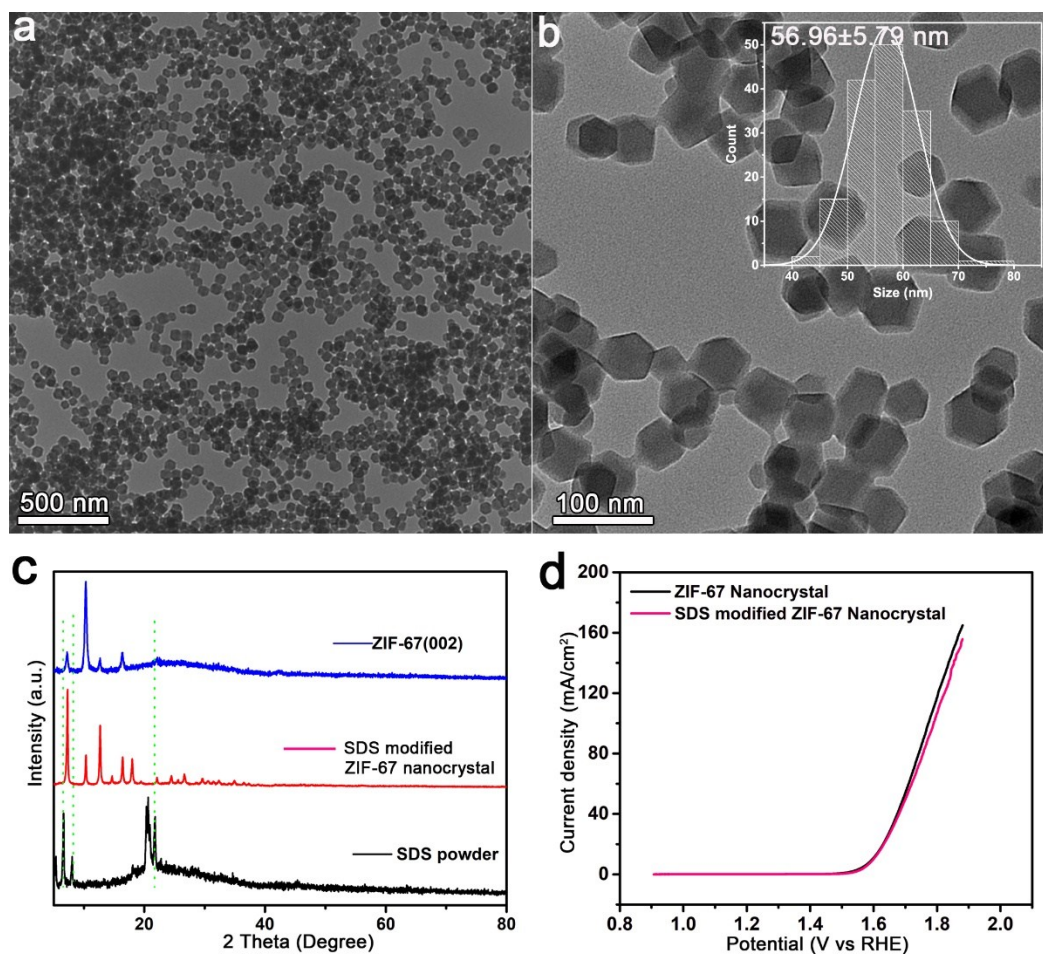


**Figure S13.** TEM results of SDS modified ZIF-67 nanocrystals. (a) TEM image at small magnification. (b) TEM image at large magnification, corresponding inset is the statistical result of nanocrystal size. (c) XRD patterns of ZIF-67 (002), SDS modified ZIF-67 nanocrystal, and pure SDS powder. (d) LSV plots of ZIF-67 nanocrystal and SDS modified ZIF-67 nanocrystal.

It should point out that the surfactants (SDS) cannot be completely removed by washing with water and ethanol. We should investigate the effect of residual SDS on OER performance. As discussed in the manuscript, the SDS helped generate the ZIF-67 (002). We could not synthesize ZIF-67 (002) without the SDS by our method. But we could design another experiment, where we synthesized SDS modified ZIF-67 nanocrystals as the sample of reference. The SDS modified ZIF-67 nanocrystal were synthesized by the following method: 1.415 g of  $\text{Co}(\text{NO}_3)_2 \cdot 6\text{H}_2\text{O}$  and 100 mg of SDS was dissolved in 100 ml ultrapure water (solution 1). Then, 1.6 g of 2-MIm was dissolved in another 100 ml ultrapure water (solution 2). Then, the two solutions were mixed together under strongly stirring. After an hour reaction, the product was

collected with centrifugation and washed with deionized water and ethanol for three times, respectively.

**In Figure S13a and S13b**, SDS modified ZIF-67 nanocrystals possessed the same morphology structure as the ZIF-67 nanocrystals. And the average diameter size of SDS modified ZIF-67 nanocrystals was  $56.96 \pm 5.79$  nm. In addition, we performed the XRD of ZIF-67 (002), SDS modified ZIF-67 nanocrystals and pure SDS powder in **Figure S13c**. Judged by the green lines in **Figure S13c**, we found no signal of SDS in ZIF-67 (002) and SDS modified ZIF-67 nanocrystals. Therefore, we concluded that there was very little SDS powder left on the surface of ZIF-67 (002) and SDS modified ZIF-67 nanocrystals. To verify the effect of residual SDS on the OER performance, OER tests with the ZIF-67 nanocrystal and SDS modified ZIF-67 nanocrystals were performed at the same condition as previous experiment. The LSV plots were displayed in **Figure S13d**, where SDS modified ZIF-67 nanocrystals demonstrated almost the same performance as pure ZIF-67 nanocrystals. At least, SDS had no positive effect on OER performance.

In summary, SDS had no positive effect on OER performance in the experiment.

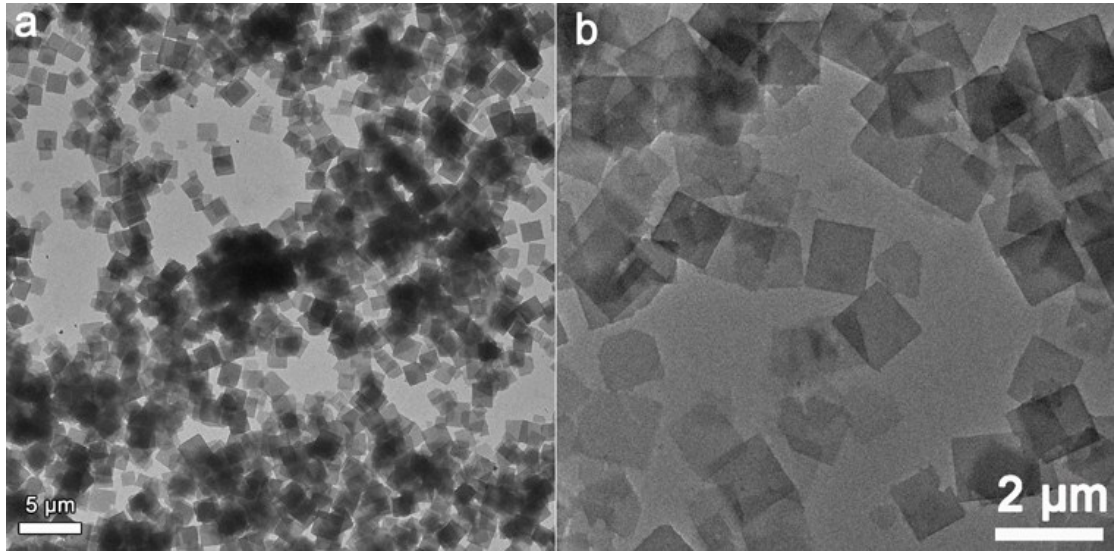


**Figure S14.** Overall TEM image (a) and local TEM image (b) of 2D ZIF-67 (002) after CA test.

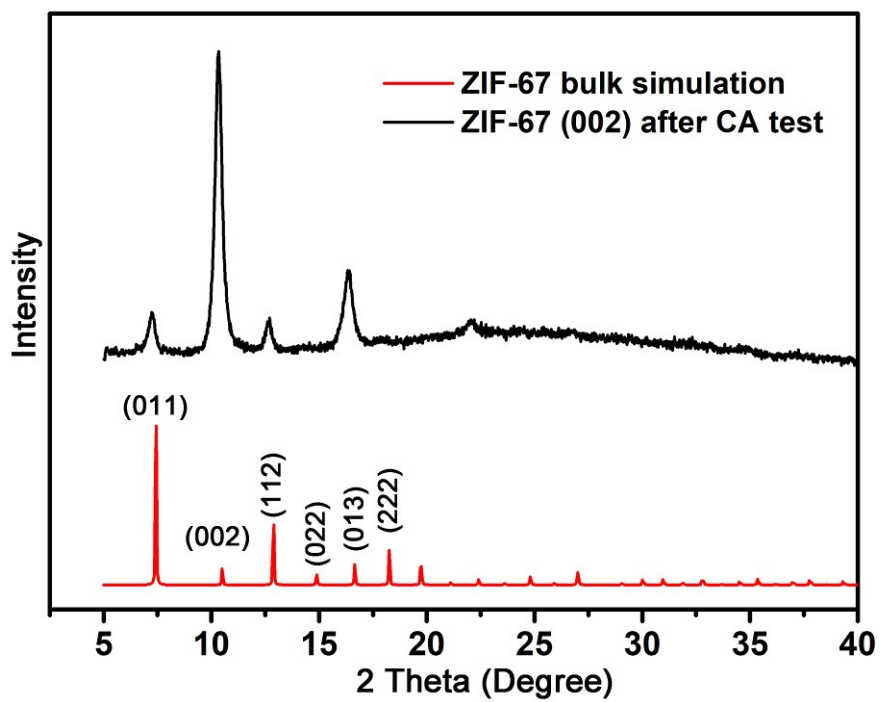


**Figure S15.** XRD pattern for 2D ZIF-67 (002) after CA test.

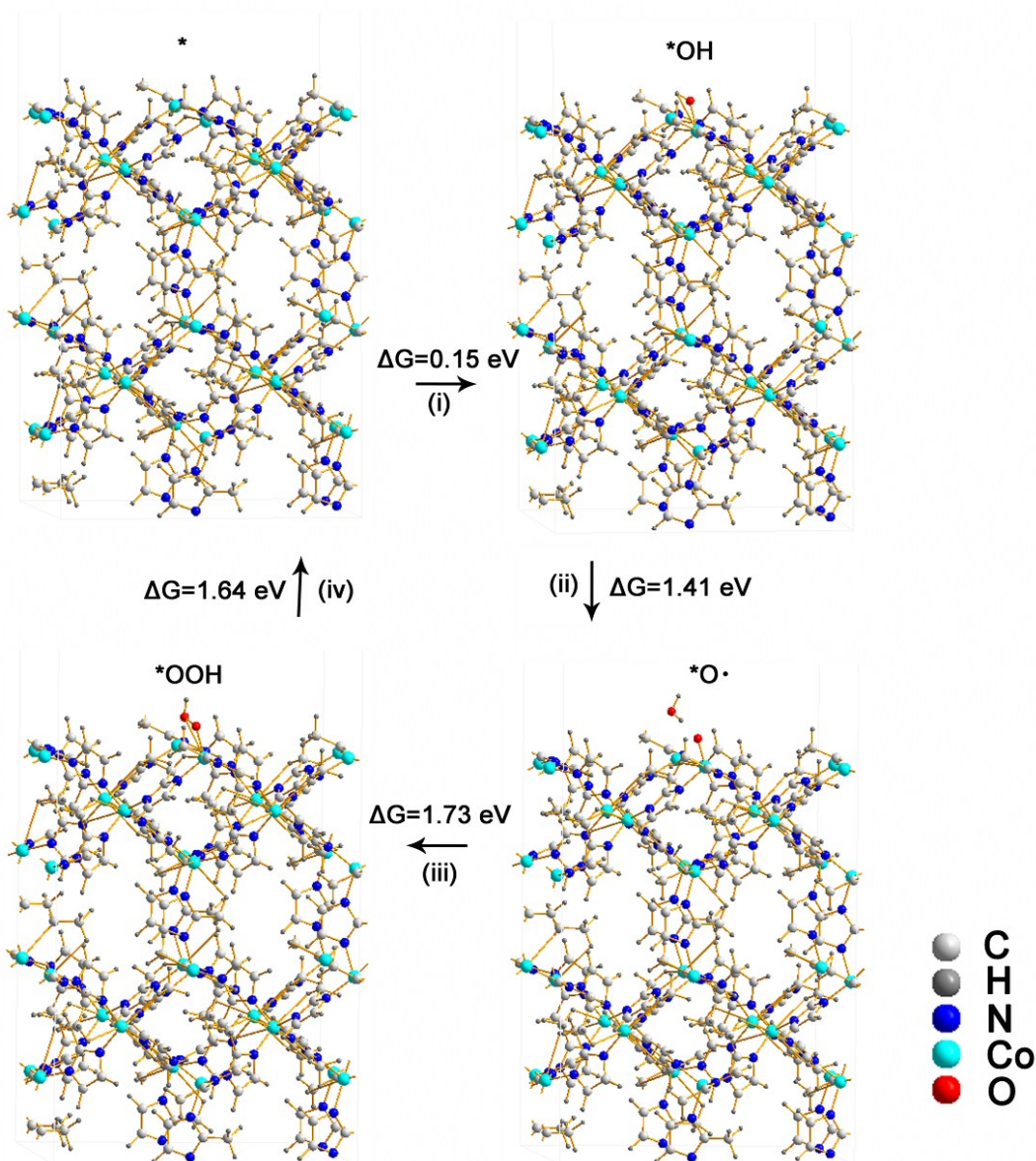


**Figure S16.** DFT calculation result of (011) facet in ZIF-67 for OER process.

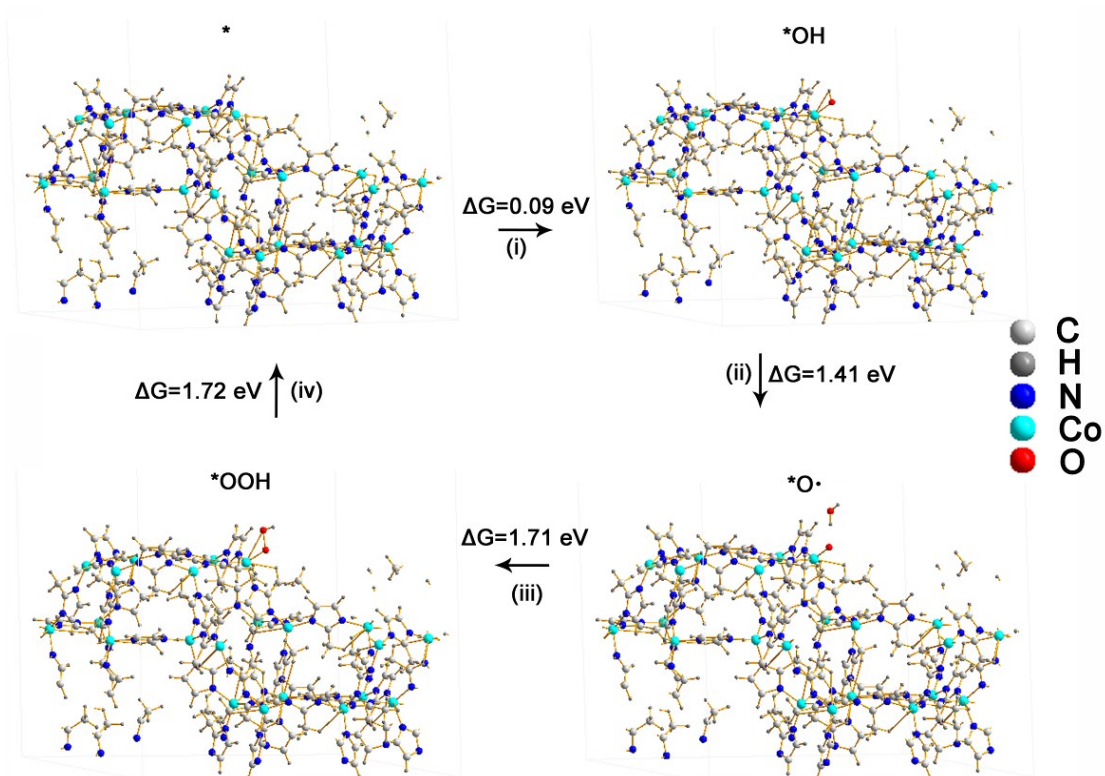


**Figure S17.** DFT calculation result of (111) facet in ZIF-67 for OER process.



**Figure S18.** 2D ZIF-67 (002) nanosheets were synthesized in large quantities.

First, 1.6 g SDS was completely dissolved in 180 ml ultrapure water under strongly stirring, followed by adding with 1.415 g  $\text{Co}(\text{NO}_3)_2 \cdot 6\text{H}_2\text{O}$ . Then, 3.195 g of 2-MIm was well dispersed in 20 ml ultrapure water. Next, the solution of 2-MIm was rapidly injected into the mixture solution. After one-hour reaction, the product was collected with centrifugation and washed with deionized water and ethanol for three times, respectively. The powder was collected by freeze-drying method. The yield of  $\sim 67.8\%$  is calculated through dividing the mass of obtained samples (3.12 g) by the theoretical production mass (4.6 g), which can be calculated from the molar amounts of precursors.



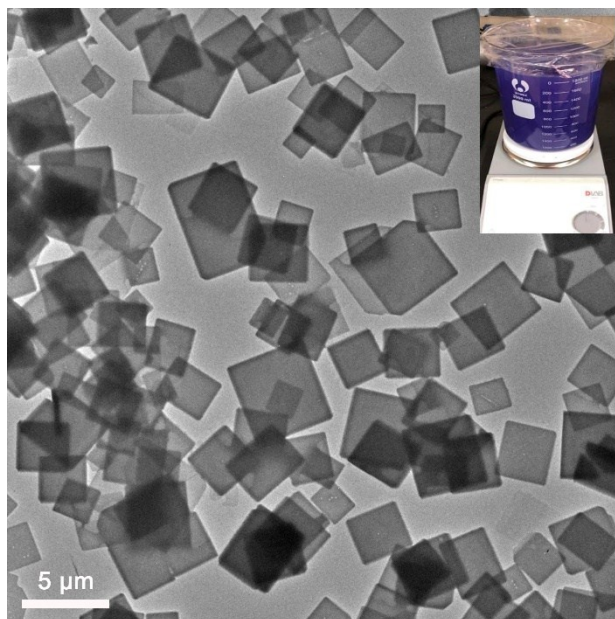


**Figure S19.** TEM image of 2D ZIF-67 by scaling-up production and inset is the corresponding synthesis process.

The reaction system expanded ten times with a 2000 ml beaker and the TEM (Figure S19) and XRD result (Figure S20) exhibited the ZIF-67 (002) structure.

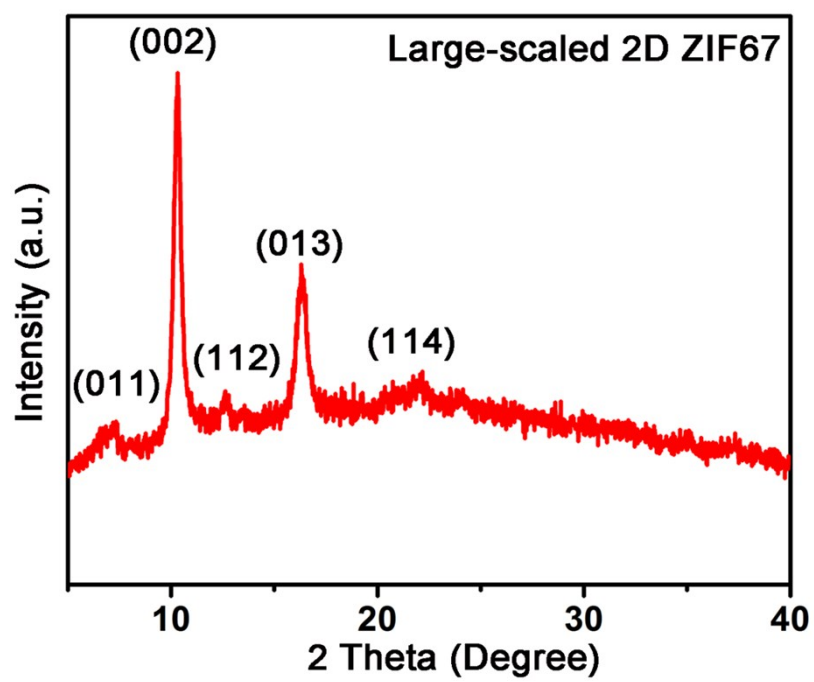


**Figure S20.** XRD result of 2D ZIF-67 by scaling-up production.

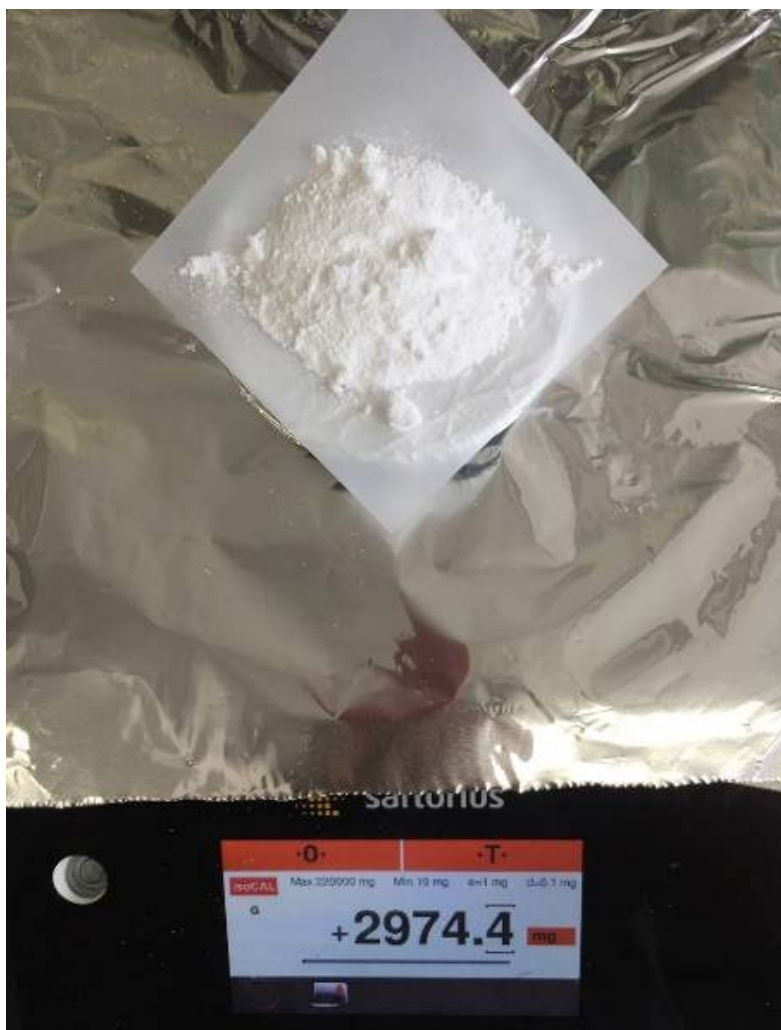


**Figure S21.** The 2D ZIF-8 (002) nanosheets were synthesized in large quantities.

First, 1.6 g SDS was completely dissolved in 180 ml ultrapure water under strongly stirring, followed by adding with 1.446 g  $\text{Zn}(\text{NO}_3)_2 \cdot 6\text{H}_2\text{O}$ . Then, 3.195 g of 2-MIm was well dispersed in 20 ml ultrapure water. Next, the solution of 2-MIm was rapidly injected into the mixture solution. After one-hour reaction, the product was collected with centrifugation and washed with deionized water and ethanol for three times, respectively. The powder was collected by freeze-drying method.

**Table S1.** The adsorption energies and stability of surface site with DFT calculations, in which the SDS is approximated by  $\text{CH}_3\text{SO}_3\text{H}$  for the compromise with computational cost.

Surfaces	Adsorption energies (eV)	Energies cost (eV/site)
002	-0.43	0.91
011	-0.25	0.93
111	-0.48	0.94

We estimated the adsorption energies of SDS on (002), (011) and (111) surfaces of ZIF-67 with DFT calculations, in which the SDS is approximated by  $\text{CH}_3\text{SO}_3\text{H}$  for the compromise with computational cost. We found that both (002) and (111) surfaces of ZIF-67 bind  $\text{CH}_3\text{SO}_3\text{H}$  strongly with adsorption energies of 0.43 and 0.48 eV, respectively, while the (011) surface bind  $\text{CH}_3\text{SO}_3\text{H}$  weakly with an adsorption energy of 0.25 eV. Additionally, the stability of surface site also contributes here: it costs 0.97, 0.96 and 0.98 eV per site to expose (002), (011) and (111) bare surface site without adsorption of SDS, respectively, but with adsorption of  $\text{CH}_3\text{SO}_3\text{H}$  (at a coverage of 1/8), it costs 0.91, 0.93 and 0.94 eV per site to expose (002), (011) and (111) surface site, respectively. Thus, the (002) surface of ZIF-67 becomes the most stable upon the adsorption of  $\text{CH}_3\text{SO}_3\text{H}$ , which indicates the most stable of (002) facet in 2D ZIF-67 upon the adsorption of SDS.

**Table S2.** DFT calculation results (in eV) for OER on facets of (002), (011), and (111) in ZIF-67.

Facet	* → *OH	*OH → *O	*OH → *OOH	*OOH → *	$\eta$
	(i)	(ii)	(iii)	(iv)	
002	0.15	1.39	1.71	1.66	0.48
011	0.15	1.41	1.73	1.64	0.50
111	0.09	1.41	1.71	1.72	0.49

where the red value marks the potential limiting step.

The predicted overpotentials ( $\eta$ 's) show that the (002) facet does deliver better OER performance than the other two.

## References

- 1 G. Kresse and J. Hafner, *Phys. Rev. B* 1993, **47**, 558-561.
- 2 G. Kresse and J. Furthmuller, *Comput. Mater. Sci.* 1996, **6**, 15-50.
- 3 G. Kresse and J. Furthmuller, *Phys. Rev. B* 1996, **54**, 11169-11186.
- 4 J. P. Perdew, K. Burke and M. Ernzerhof, *Phys. Rev. Lett.* 1996, **77**, 3865-3868.
- 5 G. Kresse and D. Joubert, *Phys. Rev. B* 1999, **59**, 1758-1775.
- 6 H. Xiao, T. Cheng, W. A. Goddard and R. Sundararaman, *J. Am. Chem. Soc.* 2016, **138**, 483-486.
- 7 H. Xiao, T. Cheng and W. A. Goddard, *J. Am. Chem. Soc.* 2017, **139**, 130-136.